Anchor University Journal of Science and Technology (AUJST)
A publication of the Faculty of Natural, Applied and Health Science, Anchor University Lagos
URL: journal.aul.edu.ng
In AJOL: https://www.ajol.info/index.php/aujst
Vol. 5 No 1, August 2024, Pp. 71-82
ISSN: 2736-0059 (Print); 2736-0067 (Online)

Analyzing Specific Attenuation for Free Space Optical Communication Across Nigerian Regions

Emmanuel I.[1*], Adedayo K.D.[1], Ikuemuya E.O.[1]
[1]Department of Physics, The Federal University of Technology, Akure
Corresponding authors email: iemmanuel@futa.edu.ng

Submitted 26 May 2024
Accepted 13 June 2024

Competing Interests.
The authors declare no competing interests.

ABSTRACT

This study investigates specific attenuation variation across Nigeria's geo-climatic regions at 780 nm, 850 nm, and 1550 nm wavelengths, using ten years of daily weather data. The analysis reveal an exponential attenuation decrease with increased visibility. In coastal areas, Lagos peaks at 60 dB/km at 0.4 km visibility, while Calabar reaches 7 dB/km at lower wavelengths, dropping to 4.8 dB/km at 1550 nm. In the Tropical Rainforest, Ibadan mirrors Lagos trends. Guinea Savannah sees 5 dB/km to 36 dB/km attenuation, with higher values in Zaria and Jos. Sahel-Sudan Savannah shows 12 dB/km to 30 dB/km, with faster attenuation at 1550 nm. Spatially, Maiduguri and Jos suffer most during fog, while Gombe fares worst during haze. Furthermore, clear conditions exhibit low attenuation. Higher wavelengths, particularly 1550 nm, show less attenuation, suggesting their suitability for optical communication in diverse Nigerian climates.

Keywords: Specific Attenuation, Geo-climatic, Optical Communication, Visibility

1. INTRODUCTION

The Free Space Optical (FSO) communication system is a technology that transmits data through the propagation of infrared light in free space (Singhal et al., 2015). This system consists of optical transceivers at both ends, enabling bidirectional communication. One of the primary challenges in free-space optical communications is atmospheric attenuation, which can result in signal loss and link failures (Kaushal et al., 2015). The atmosphere attenuates the light wave and introduces distortion and bending. Various factors such as scattering and turbulence affect the signal's transmitted power, leading to fluctuations in the received signal quality. Attenuation in FSO systems occurs primarily due to absorption and scattering by molecules and suspended particles (aerosols) in the atmosphere

https://dx.doi.org/10.4314/aujst.v5i1.7

(Maswikaneng *et al*., 2022; Alkholidi and Altowij, 2012). However, distortion is caused by atmospheric turbulence, which results from fluctuations in the index of refraction (Yasarla and Patel, 2021).

Previous studies examined the impact of various atmospheric conditions on FSO communications. For instance, Datch et al. (2019) explored the effects of weather conditions such as rain, fog, and haze on FSO links, identifying significant signal degradation during adverse weather. Similarly, Majumdar and Ricklin (2008) provided a comprehensive analysis of optical wave propagation in the atmosphere, highlighting the factors influencing signal attenuation and distortion. Despite these efforts, there remains a gap in the literature regarding the spatial distribution and specific attenuation characteristics across different climatic regions, particularly in diverse environments such as Nigeria.

In radio system design, accurate prediction of the impact of atmospheric variables such as rain, mist, clouds, and refractive index fluctuations is vital (Ghalot et al., 2019). These factors can cause attenuation and interfere with various forms of communication, including remote, mobile, and satellite communications (Fahey et al., 2021). Rainfall-induced signal attenuation, commonly known as rain fade, affects microwave communication systems operating at frequencies above 10 GHz. However, visibility also plays a crucial role in optical communication. Reduced visibility due to fog, mist, or haze increases the scattering and absorption of light, leading to signal loss. As visibility decreases, the effective path length for optical signals grows, resulting in higher attenuation. Fog events and strong snow events are the most adverse weather conditions because they result in high specific attenuation to optic waves.

Study Locations

Nigeria approximately lies between latitude 4^o N and 14^o N and longitude 3^o E and 15^o E and occupies an area approximately 923,768 km^2. It is bounded in the south and west by the Atlantic Ocean and Benin republic respectively. The northern and eastern part share border with Niger republic and Cameroun Mountain to Lake Chad respectively. The climate of West Africa is characterized by wet and dry seasons (Barry *et al*., 2018). This work covered fifteen locations across Nigeria, classified into Coastal, Tropical rain forest, Guinea savannah and Sahel -Sudan savannah region, based on the work of Akinsanola and Ogunjobi, (2014), as shown in Figure 1.

Data Source and Analysis

Ten years (2011-2020) daily visibility, temperature, wind speed and relative humidity data for fifteen locations across Nigeria were obtained from the Iowa Environmental Mesonat (IEM) archive. The archive aggregates historical weather observation from Unidata Integrated Data Viewer (IDD), National centers for Environmental information (NCEI), Integrated Surface data (ISD), and Meteoro-logical Association Data Ingest System (MADIS).

The specific attenuation, A, in dB/km was calculated from the obtained visibility data using (Esmail *et al*., 2019):

https://dx.doi.org/10.4314/aujst.v5i1.7

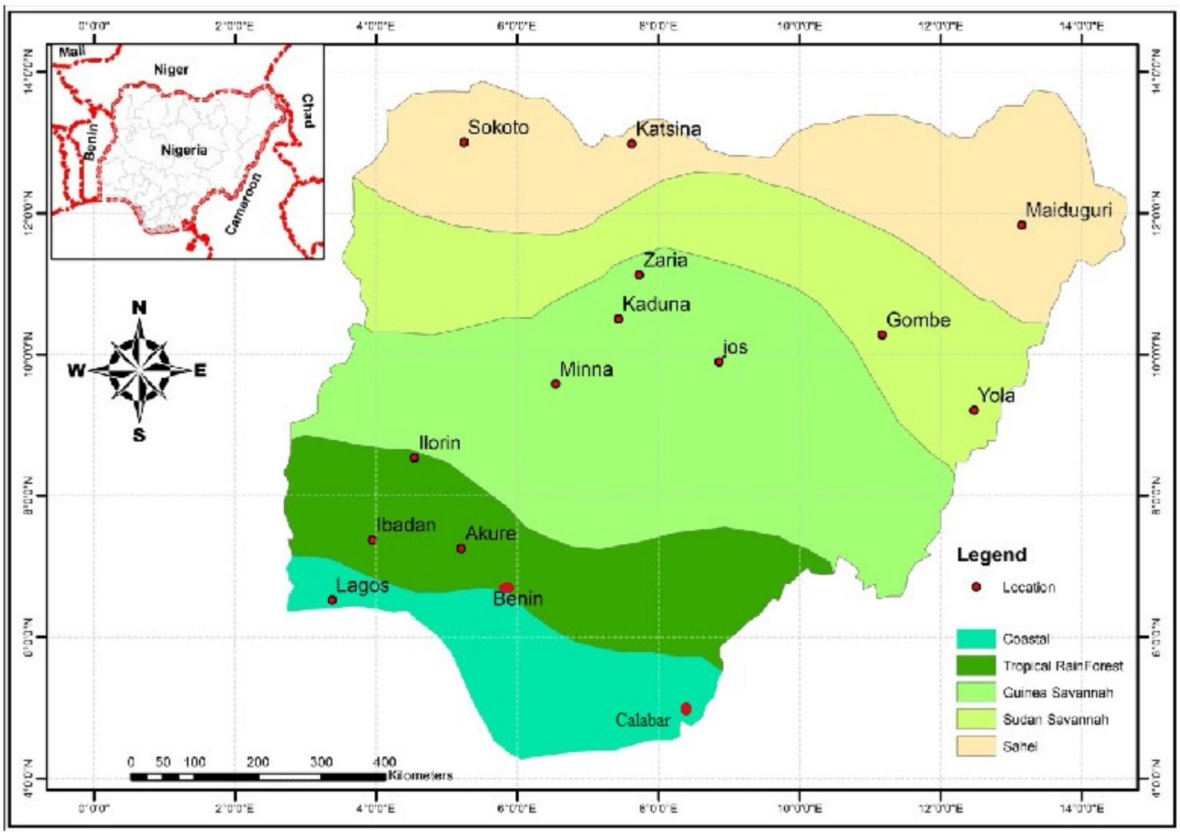

Figure 1: Map showing study locations.

$$A\left(\frac{dB}{km}\right) = 10\log_e \gamma(\lambda) \quad (1)$$

$$\gamma(\lambda) = \frac{3.91}{V}\left(\frac{\lambda}{550\ nm}\right)^{-p} \quad (2)$$

where V is the visibility range and λ is the operating wavelength, p is the size distribution coefficient that describes the "thickness" of the fog, γ is the attenuation coefficient, 550 nm is the reference wavelength used in this approach. The Kruse model defines p for different visibility factors using (Corrigan *et al.*, 2009): :

$$p = \begin{cases} 1.6, & V > 50 \\ 1.3, & 6 < V < 50 \\ 0.585V^{1/3}, & V < 6 \end{cases} \quad (3)$$

Atmospheric attenuation τ(R) was calculated using Beers-Lambert law given as (Oshina and Spigulis, 2021):

$$\tau(R) = -\frac{P(R)}{P(O)} = \log(-\gamma R \quad (4)$$

where τ(R) is transmittance at distance R; P(R) is received signal power; P(0) is transmitted signal power and R is link distance in, therefore:

$$\tau(R) = \log_e\left[\left(\frac{3.91}{V}\right) * \left(\frac{\lambda}{550nm}\right)^{-p} * R\right] dB \quad (5)$$

Results and Discussion

Specific Attenuation as a Function of Visibility Variations of specific attenuation at three different operating wavelengths (780

https://dx.doi.org/10.4314/aujst.v5i1.7

Table 3.1: Showing Weather Conditions with their corresponding Visibility values (Subekti *et al*., 2020)

Weather Conditions	Visibility
Foggy	Less than 1 km
Hazy	Between 1km to 6 km
Clear Weather	Greater than 6 km

nm, 850 nm, and 1550 nm) as a function of visibility were evaluated and observed across the four geo-climatic regions of Nigeria. Figures (2 - 5) represent the variation of specific attenuation as a function of visibility in the Coastal, Tropical rainforest, Guinea savannah, Sahel, and Sudan savannah regions respectively. The variation of the specific attenuation decreases exponentially with an increase in visibility in all the observed locations across the regions.

In Coastal regions, the values of specific attenuation reach a maximum value of 60 dB/km at 0.4 km visibility in Lagos (Figure 2a). It decreases slightly and approaches zero at a visibility of 2 km. The variation of specific attenuation at Calabar is slightly different from that of Lagos. Specific attenuation reached its maximum values of 7 dB/km at operating wavelength of 780 nm and 850 nm. However, as the operating wavelength increases, the specific attenuation decreases with a value of 4.8 dB/km (Figure 2b). Similarly, the specific attenuation decreases with increase in visibility with the values of specific attenuation at 1550 nm operating wavelength lagging the 780 nm, 850 nm operating wavelength. Unlike Lagos, the values of specific attenuation here approach zero at visibility of 7.0 km. Generally, specific attenuation reduces as operating wavelength increases. The variation of the specific attenuation at Tropical Rain Forest is presented in Figure 3. In this region, the values of specific attenuation variation follow similar trend like that of Lagos.

In Ibadan, maximum specific attenuation of 38 dB/km is observed at 0.4 km visibility, while at Akure and Benin, 35 dB/km maximum specific attenuation is observed at 0.8 km visibility. Specific attenuation at Akure and Benin follow similar trend with little deviation as shown in Figure 3. The values of specific attenuation decay rapidly at 1550 nm operating wavelength than 780 nm and 850 nm operating wavelength. The values of specific attenuation approach zero at 6 km visibility for 1550 nm operating wavelength, similarly, it approaches zero at 8 km visibility for 780 nm and 850 nm operating wavelength. Unlike other station, the values of the specific attenuation at the three wavelength approaches zero at 2 km visibility in Ibadan.

In Guinea savannah region which comprises Ilorin, Jos, Kaduna, Zaria and Yola, the maximum values of the specific attenuation vary between 5 dB/km and 36 dB/km, (Figure 4). Maximum value of 5 dB/km associated with operating wavelength of 780 nm and 850 nm at

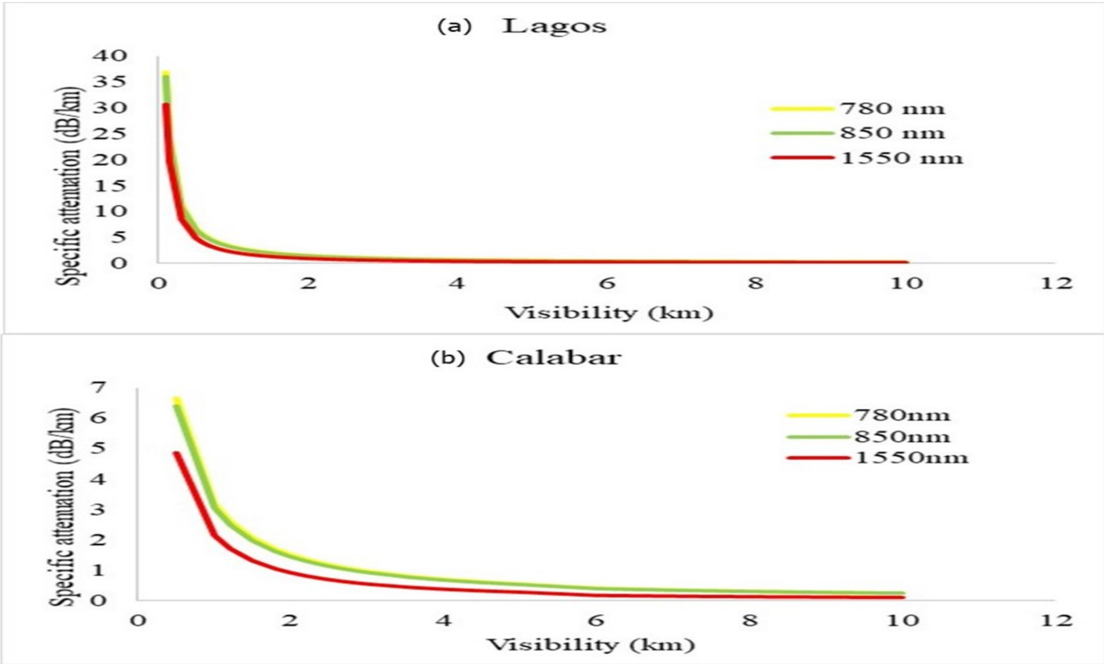

Figure 2: Variation of specific attenuation as a function of visibility in Coastal region

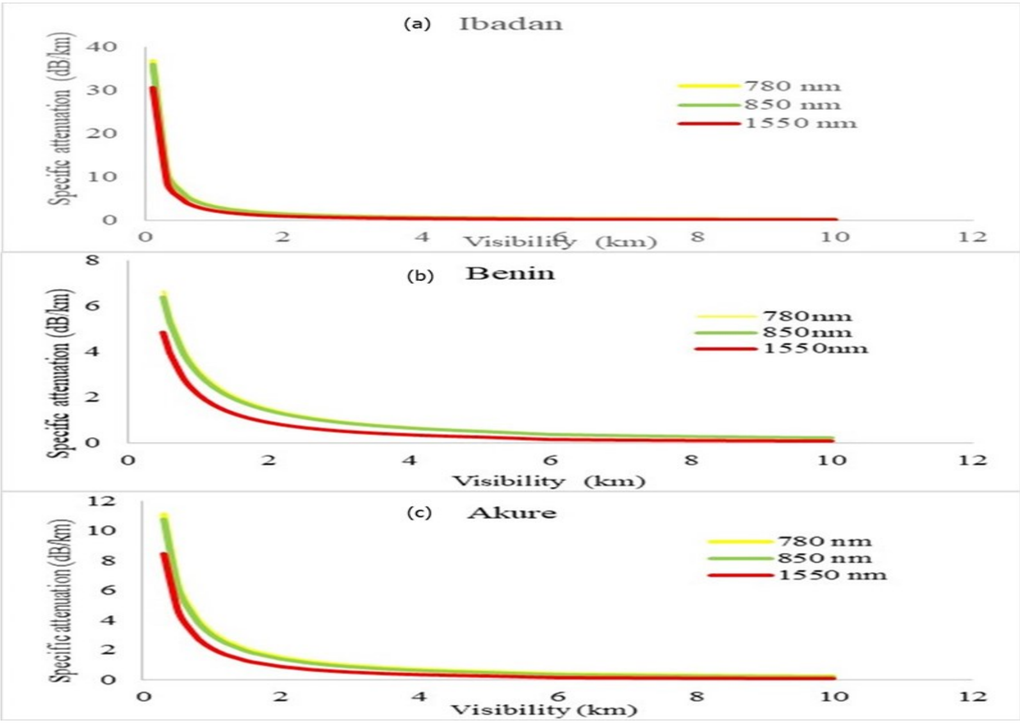

Figure 3: Variation of specific attenuation as a function of visibility in Tropical rainforest region

visibility of 2 km is observed in Zaria whereas at 1550 nm operating wavelength, the maximum value is 35 dB/km at 1.8 km visibility. The trend of the specific attenuation at Jos and Kaduna are similar with minor variation. The maximum value of 35 dB/km of the three operating wavelengths was noticed in Jos at 0.8 km visibility. At Kaduna, the maximum of 30 dB/km at 0.6 km visibility was observed at all the operating wavelength. In Ilorin and Yola, maximum specific attenuation values were 11 dB/km and 18 dB/km respectively, at 1 km visibility with the values of specific attenuation tending to zero at visibility of 8 km for Ilorin and 6 km visibility for Yola. In the Sahel-Sudan savannah climatic region (Figure 5), the maximum specific attenuation

https://dx.doi.org/10.4314/aujst.v5i1.7

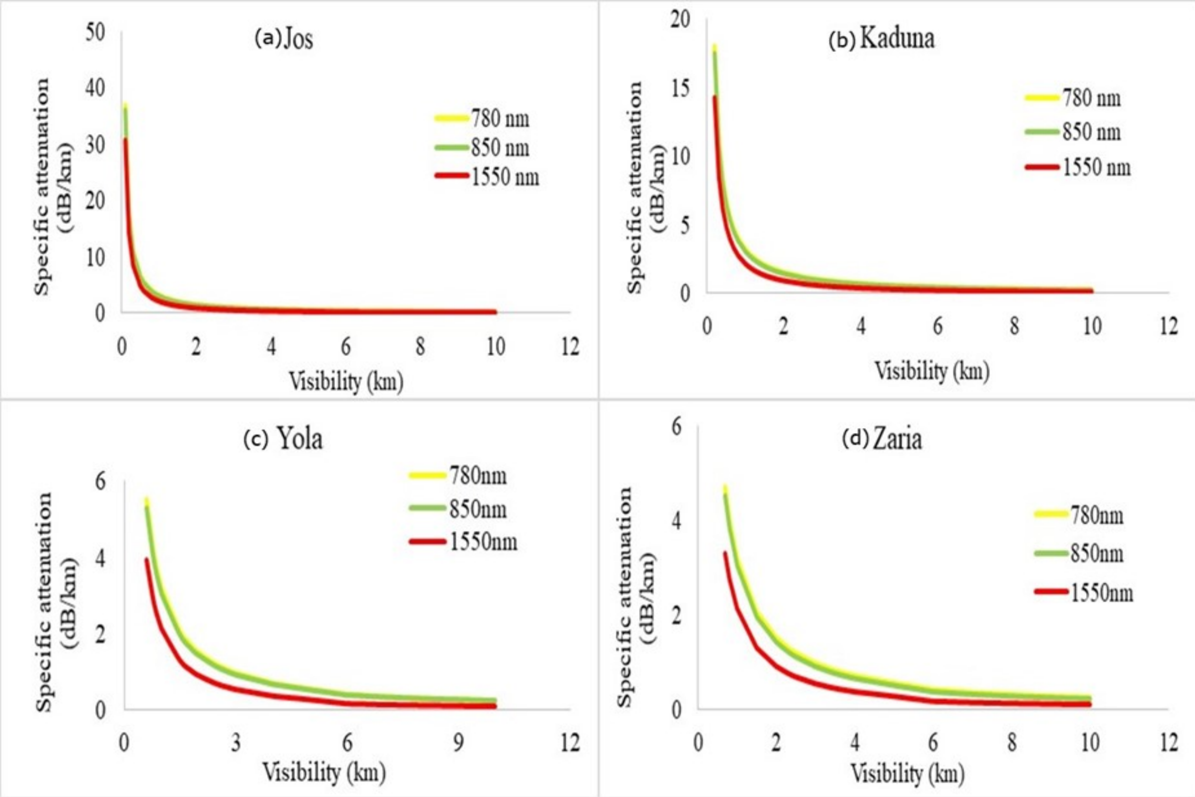

Figure 4: Variation of specific attenuation as a function of visibility in Guinea Savannah region

value for Gombe was 12 dB/km for operating wavelength of 780 nm and 850 nm while 8 dB/km for 1550 nm operating wavelength, the 1550 nm wavelength experience less attenuation and it lags behind the other two operating wavelength. When the visibility was around 6 km, the specific attenuation approaches zero. Specific attenuation variation with visibility in Maiduguri, Sokoto and Katsina follows almost similar trend with maximum value of specific attenuation for Katsina being 30 dB/km at a visibility of 1 km for 780 nm and 850 nm operating wavelengths and 18 dB/km for Sokoto and Maiduguri at same visibility of 1 km. The 1550 nm operating wavelength experiences lesser attenuation when compared to the other wavelengths in all the locations under this climatic zone, from visibility of 4 km for Sokoto and Maiduguri, the specific approaches zero while for Katsina the attenuation value approaches zero from 3 km visibility. In this region-specific attenuation decreases rapidly and its value tend to zero at 6 km visibility. At operating wavelength of 1550 nm, the attenuation tends to zero faster than other operating wavelength. At an operating wavelength of 1550 nm, the reduced attenuation implies more efficient propagation of optical signals over longer distances compared to 850 nm and 780 nm wavelengths (Sahoo and Yadav, 2024).

Spatial Distribution of Specific Attenuation under Different Weather Condition

The distribution of specific attenuation over Nigeria during foggy, hazy and clear weather conditions at different operating wavelength are presented using spatial distribution obtained from Kriging interpolation method (Figure 6). During foggy condition (Figure 7a), the values of the specific attenuation oscillate between 0 and 7 dB/km at operating wavelength of 780 nm. The highest value of 7 dB/km specific attenuation was observed in part of Maiduguri and Jos, the lowest value of 0.001 dB/km was noticed in Sokoto. This

https://dx.doi.org/10.4314/aujst.v5i1.7

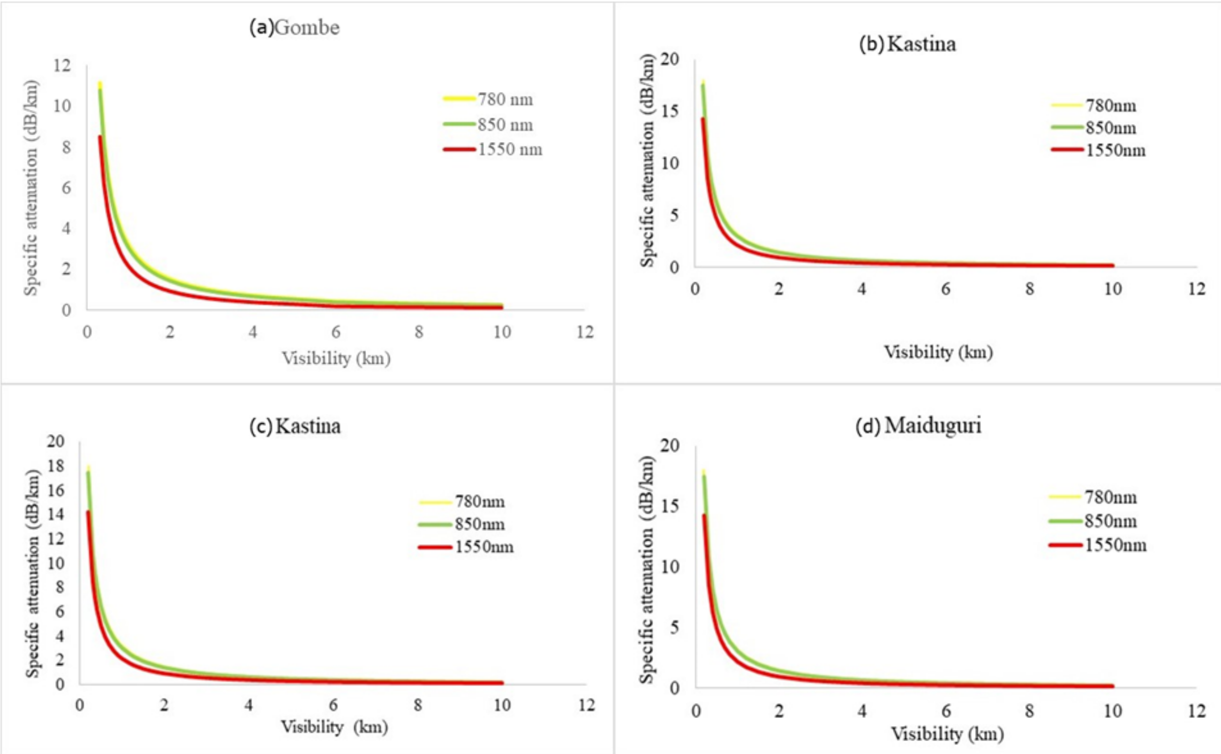

Figure 5. Variation of specific attenuation as a function of visibility in Sahel- Sudan Savannah region

variation may be attributed to the altitude and meteorological condition of the locations (Akpootu *et al*., 2023). At 850 nm and 1550 nm operating wavelength, the variation of the specific attenuation across Nigeria follows similar pattern as that of 780 nm. It is worth noting that the values of specific attenuation ranges from 0 dB/km to 6.7 dB/km and 0 dB/km to 5.2 dB/km at 850 nm and 1550 nm operating wavelength respectively. Likewise, the variation of specific attenuation during hazy condition (Figure 7b), follows the same pattern as that of foggy condition. However, during this condition, the values of specific attenuation vary between 0.5 dB/km and 1.37 dB/km. The highest values of specific attenuation were noticed at Gombe while the lowest was observed in Sokoto and Akure. The variation of specific attenuation at operating wavelength of 850 nm and 1550 nm follows similar pattern as 780 nm under the hazy condition with values of specific attenuation ranging from 0.47 dB/km to 1.29 dB/km and 0.25 dB/km to 0.83 dB/km for 850 nm and 1550 nm respectively. Likewise, the variation of specific attenuation during hazy condition (Figure 7b), follows the same pattern as that of foggy condition. However, during this condition, the values of specific attenuation vary between 0.5 dB/km and 1.37 dB/km. The highest values of specific attenuation were noticed at Gombe while the lowest was observed in Sokoto and Akure. The variation of specific attenuation at operating wavelength of 850 nm and 1550 nm follows similar pattern as 780 nm under the hazy condition with values of specific attenuation ranging from 0.47 dB/km to 1.29 dB/km and 0.25 dB/km to 0.83 dB/km for 850 nm and 1550 nm respectively. Also, for

https://dx.doi.org/10.4314/aujst.v5i1.7

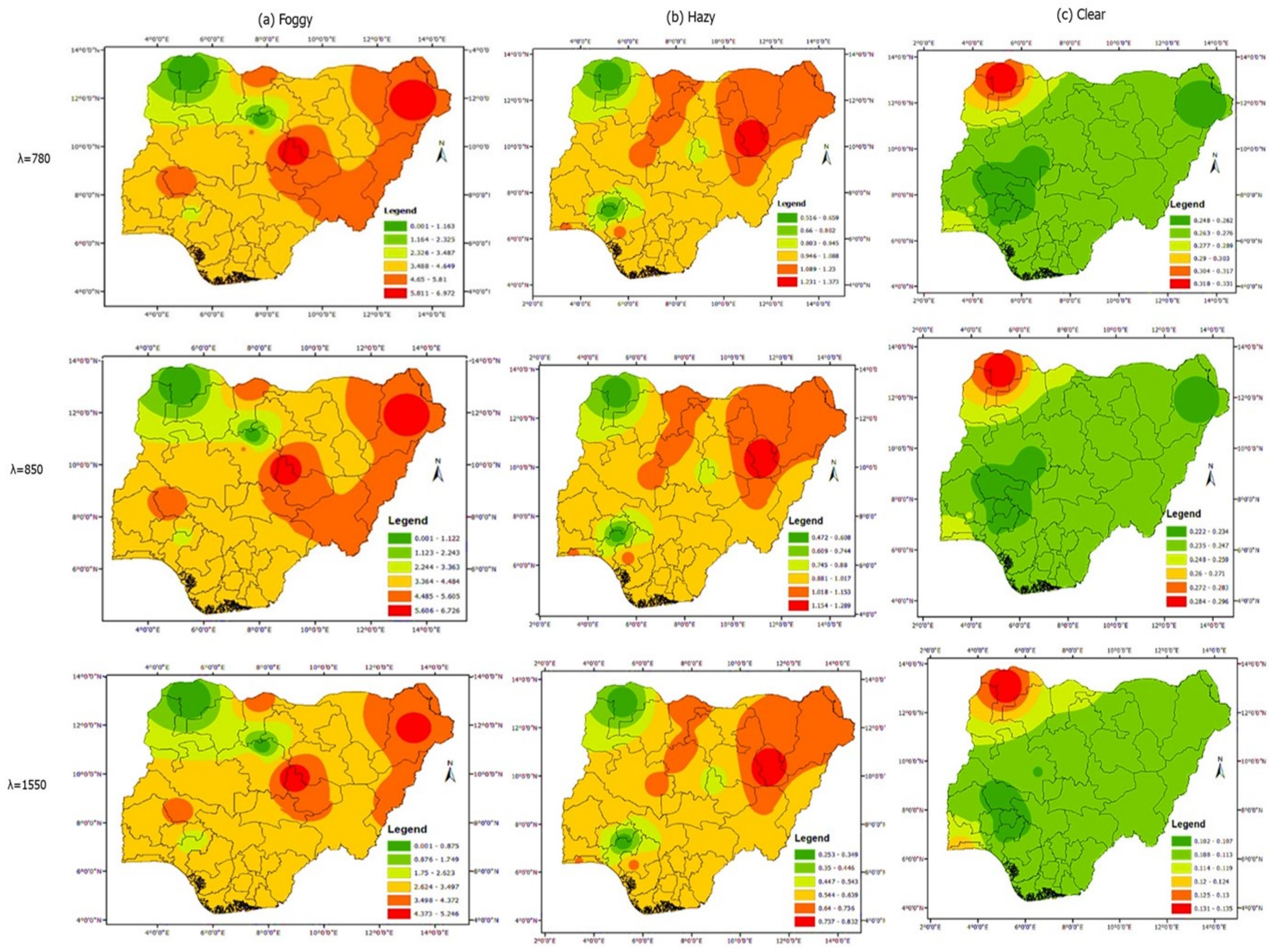

Figure 6: Spatial distribution of specific attenuation under different weather condition

for clear air condition (Figure 7c), where visibility value is greater than 6 km specific attenuation value for 780 nm and 850 nm was approximately around 0.2 dB/km to 0.3 dB/km showing very low attenuation with the highest value of specific attenuation occurring in Sokoto. For 1550 nm operating wavelength, the specific attenuation value ranges between 0.1 dB/km and 0.14 dB/km, this also represent a low attenuation of signals across all locations under this wavelength in clear air condition. This implied that Maiduguri and Jos are most prone to the highest attenuation during foggy conditions and Gombe during hazy conditions. This means that during foggy conditions, optical signals in Maiduguri and Jos will suffer greater attenuation, while Gombe will experience higher attenuation during hazy conditions, potentially affecting communication and visibility (Singh and Mittal, 2022). This could lead to disruptions in communication networks and transportation, increasing the risk of accidents and reducing the effectiveness of emergency services (Rak *et al.,* 2021).

Conclusion

This study investigated the variations in specific attenuation across Nigeria's geo-climatic regions and under different visibility conditions. The analysis highlights the importance of considering operating wavelengths, with higher

https://dx.doi.org/10.4314/aujst.v5i1.7

wavelengths, notably 1550 nm, experiencing less attenuation. Coastal regions exhibit distinct attenuation patterns, with Lagos and Calabar showcasing differing trends. Similarly, the Tropical Rainforest region demonstrates attenuation behaviors akin to coastal areas, particularly in Ibadan. In contrast, the Guinea Savannah and Sahel-Sudan Savannah regions display unique attenuation profiles, with notable variations across locations. Spatially, Maiduguri and Jos emerge as particularly susceptible to high attenuation during fog, while Gombe experiences heightened attenuation during haze. Clear weather conditions consistently exhibit low attenuation values across all regions. These findings have significant implications for optical communication infrastructure deployment and optimization in Nigeria. Future work will investigate the impact of seasonal changes on specific attenuation patterns to improve optical communication infrastructure deployment in Nigeria.

Reference

Akinsanola, A. A., and Ogunjobi, K. O. (2014). Analysis of Rainfall and Temperature Variability Over Nigeria. 14(3).

Akpootu, D. O., Alaiyemola, S. R., Abdulsalam, M. K., Bello, G., Umar, M., Aruna, S., Isah, A. K., Aminu, Z., Abdullahi, Z., and Badmus, T. O. (2023). Sunshine and Temperature Based Models for Estimating Global Solar Radiation in Maiduguri, Nigeria. *Saudi Journal of Engineering and Technology*, *8*(05), 82–90. https://doi.org/10.36348/sjet.2023.v08i05.001

Alkholidi, A., and Altowij, K. (2012). Effect of Clear Atmospheric Turbulence on Quality of Free Space Optical Communications in Western Asia.

Barry, A. A., Caesar, J., Klein Tank, A. M. G., Aguilar, E., McSweeney, C., Cyrille, A. M., Nikiema, M. P., Narcisse, K. B., Sima, F., Stafford, G., Touray, L. M., Ayilari-Naa, J. A., Mendes, C. L., Tounkara, M., Gar-Glahn, E. V. S., Coulibaly, M. S., Dieh, M. F., Mouhaimouni, M., Oyegade, J. A., and Laogbessi, E. T. (2018). West Africa climate extremes and climate change indices. *International Journal of Climatology*, *38*, e921–e938. https://doi.org/10.1002/joc.5420

Datch, C. A. B., & Faye, N. A. B. (2019). Resilience of Long Range FSO Link under a Tropical Weather Effects. *Sci. Afr*, *7*, e00243.

Esmail, M. A., Member, S., Fathallah, H., and Member, S. (2019). An Experimental Study of FSO Link Performance in Desert Environment. *IEEE communications letters*. *March*. https://doi.org/10.1109/LCOMM.2016.2586043

Fahey, T., Islam, M., Gardi, A., and Sabatini, R. (2021). Laser beam atmospheric propagation modelling for aerospace LIDAR applications. *Atmosphere*, *12*(7), 1–47. https://doi.org/10.3390/atmos12070918

Ghalot, R., Madhu, C., Kaur, G., and Singh, P. (2019). Link estimation of different Indian cities under fog weather conditions.

Akinsanola, A. A., and Ogunjobi, K. O. (2014). Analysis of Rainfall and Temperature Variability Over Nigeria. 14(3).

Akpootu, D. O., Alaiyemola, S. R., Abdulsalam, M. K., Bello, G., Umar, M., Aruna, S., Isah, A. K., Aminu, Z., Abdullahi, Z., and Badmus, T. O. (2023). Sunshine and Temperature Based Models for Estimating Global Solar Radiation in Maiduguri, Nigeria. *Saudi Journal of Engineering and Technology*, *8*(05),

82–90. https://doi.org/10.36348/sjet.2023.v08i05.001

Alkholidi, A., and Altowij, K. (2012). Effect of Clear Atmospheric Turbulence on Quality of Free Space Optical Communications in Western Asia.

Barry, A. A., Caesar, J., Klein Tank, A. M. G., Aguilar, E., McSweeney, C., Cyrille, A. M., Nikiema, M. P., Narcisse, K. B., Sima, F., Stafford, G., Touray, L. M., Ayilari-Naa, J. A., Mendes, C. L., Tounkara, M., Gar-Glahn, E. V. S., Coulibaly, M. S., Dieh, M. F., Mouhaimouni, M., Oyegade, J. A., and Laogbessi, E. T. (2018). West Africa climate extremes and climate change indices. *International Journal of Climatology*, *38*, e921–e938. https://doi.org/10.1002/joc.5420

Datch, C. A. B., & Faye, N. A. B. (2019). Resilience of Long Range FSO Link under a Tropical Weather Effects. *Sci. Afr*, *7*, e00243.

Esmail, M. A., Member, S., Fathallah, H., and Member, S. (2019). An Experimental Study of FSO Link Performance in Desert Environment. *IEEE communications letters. March*. https://doi.org/10.1109/LCOMM.2016.2586043

Fahey, T., Islam, M., Gardi, A., and Sabatini, R. (2021). Laser beam atmospheric propagation modelling for aerospace LIDAR applications. *Atmosphere*, *12*(7), 1–47. https://doi.org/10.3390/atmos12070918

Ghalot, R., Madhu, C., Kaur, G., and Singh, P. (2019). Link estimation of different Indian cities under fog weather conditions. *Wireless Personal Communications*, *105*, 1215-1234.

Kaushal, H., Kaddoum, G., and Engineering, C. (2015). Free Space Optical Communication : Challenges and Mitigation Techniques. 1–28. arXiv:1506.04836v1

Maswikaneng, S. P., Adebusola, S. O., Owolawi, P. A. and Ojo, S. O. (2022). Estimating effect of total specific atmospheric attenuation on performance of FSO communication link in South Africa. Journal of Communications; Vol. 17, Issue 7

Oshina, I., and Spigulis, J. (2021). Beer–Lambert law for optical tissue diagnostics: current state of the art and the main limitations. *Journal of Biomedical Optics*, *26*(10), 1–17. https://doi.org/10.1117/1.jbo.26.10.100901

Rak, J., Girão-Silva, R., Gomes, T., Ellinas, G., Kantarci, B., & Tornatore, M. (2021). Disaster resilience of optical networks:

State of the art, challenges, and opportunities. Optical Switching and Networking, 42, 100619.

Sahoo, P. K., & Yadav, A. K. (2024). A comprehensive road map of modern communication through free-space optics. Journal of optical communications, 44(s1), s1497-s1513.

Singh, H., & Mittal, N. (2022). Analyzing the impact of fog and atmospheric turbulence on the deployment of free-space optical communication links in India. Arabian Journal for Science and Engineering, 47(3), 2691-2710.Singh, H. H. I. M. J., Al-Bawri, S. S., Alzamil, M. T. I. A., and Islam, M. S. (2022). Radio Frequency Energy Harvesting Technologies : A Comprehensive Review on Designing Methodologies, and Potential Applications. *Sensors*. Vol. 22. 4144. https://doi.org/ 10.3390/ s22114144.

Subekti, T., Isnawati, A. F., and Zulherman, D. (2020). *Optimation Free Space Optic (FSO) Design with Kim Model Using Space Optimization Free Space Optic (FSO) Design with Kim Model Using Space Diversity*. https:// doi.org/10.20895/infotel.v11i3.444

Yasarla, R., and Patel, V. M. (2021). Learning to restore images degraded by atmospheric turbulence using uncertainty. *IEEE International Conference on Image Processing (ICIP)*, *2*.

Zhang, C., Zhang, J., Wu, X., and Huang, M. (2020). Numerical analysis of light reflection and transmission in poly-disperse sea fog. *28*(17), 25410–25430.